

VDMOS POWER TRANSISTOR DRAIN-SOURCE RESISTANCE  
RADIATION DEPENDENCE\*D. L. Blackburn,<sup>†</sup> T. C. Robbins,<sup>§</sup> and K. F. Galloway<sup>¶</sup>Abstract

Data on the effects of neutron and gamma radiation on the drain-source resistance characteristics of power VDMOS transistors are presented. The change in resistance with neutron exposure is related to the resistivity of the drain material, which in turn can be related to the drain-source breakdown voltage. A device with a 450-V rating experienced a factor of 13 increase in resistance on exposure to a neutron fluence of  $10^{14}/\text{cm}^2$  whereas one with a breakdown voltage of 150 V experiences no increase in resistance. Threshold voltage shifts of about 2 V occurred at a gamma dose of  $10^5$  rad(Si) without bias and was accelerated by positive gate bias. All of these data are consistent with the predictions of a simple model for the dependence of drain-source resistance on gate voltage and drain resistivity. This model illustrates a general separability of neutron and gamma effects on power VDMOS devices. The systems implications for using this type device in a radiation environment are briefly addressed.

Introduction

Recent advances in power MOSFET technology have opened new application areas and have increased interest in using power MOS transistors.<sup>1,2</sup> As majority-carrier devices without the minority-carrier charge storage effects of bipolar transistors, power MOSFETs are generally capable of faster switching speeds than power bipolar transistors. Also, a negative temperature coefficient of carrier mobility greatly decreases the potential for thermal runaway, second breakdown, and current hogging in power MOSFETs as compared to bipolar devices.

The effects of radiation on power MOSFETs and the effects of device design on radiation susceptibility require investigation as the application possibilities of these devices expand. Previously, data have been presented on the effects of gamma irradiation on the threshold voltage<sup>3</sup> and on the effects of a mixed gamma-neutron environment on the drain-source breakdown voltage.<sup>4</sup> This paper concentrates on the effects of radiation on power MOSFET drain-source resistance ( $R_{DS}$ ). Data on the effects of both gamma and neutron environments on this parameter and a simple model to predict the effects of radiation on  $R_{DS}$  are presented.

A number of different physical structures for power MOSFETs are currently available. For specificity, the work reported in this paper is confined to vertical double-diffused MOS (VDMOS) structures as schematically illustrated in figure 1. Double-diffusion techniques are used to achieve devices with 1- to 3- $\mu\text{m}$  channel lengths. It is expected that radiation effects will primarily manifest themselves as shifts in threshold voltage due to ionizing radiation exposure and as changes in the drain-source resistance due to neutron exposure.

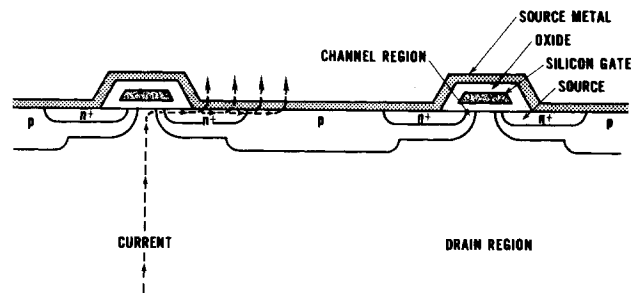


Figure 1. Schematic illustration of VDMOS device structure.

Model

For an n-channel device as shown in figure 1, the current flow is from the drain contact vertically through the drain region, then horizontally through the channel to the source region. The drain-source resistance of a VDMOS power device can be expressed as:<sup>5</sup>

$$R_{DS} = \frac{1}{(W/L) \cdot C_0 \cdot \mu_e \cdot [V_G - V_{th}]} + F \cdot \rho_D \quad (1)$$

where  $W$  is the channel width,  $L$  is the effective channel length,  $C_0$  is the gate oxide capacitance per unit area,  $\mu_e$  is the electron inversion layer mobility,  $V_G$  is the gate voltage,  $V_{th}$  is the threshold voltage,  $\rho_D$  is the resistivity of the drain region material, and  $F$  is a geometrical factor depending only on the device dimensions. The possible effect of the enhancement region at the drain surface beneath the gate<sup>5</sup> and any effect of the source region resistance have been neglected. Also, any dependence of  $\mu_e$  on  $V_G$  has been neglected.

The first term in equation 1 is the resistance of the channel region, and the second term is the resistance of the drain region. A plot of  $R_{DS}$  versus gate voltage for a typical VDMOS device as predicted by equation 1 is shown in figure 2.

After exposure of the device to a mixed gamma and neutron radiation environment, the  $R_{DS}$  versus  $V_G$  relationship shifts both vertically and laterally as indicated by the arrows in figure 2. It is well known that the principal effect of gamma irradiation is to lower the value of  $V_{th}$  by the introduction of gate-oxide charge. This causes the  $R_{DS}$  versus  $V_G$  curve to shift laterally to the left to smaller values of  $V_G$ . The effect of ionizing radiation on  $\mu_e$  has been ignored, and it is not expected that ionizing irradiation should affect the other parameters in equation 1.

\* Contribution of the National Bureau of Standards. Not subject to copyright.

<sup>†</sup> D. L. Blackburn is with the Semiconductor Devices and Circuits Division, National Bureau of Standards, Washington, DC 20234.

<sup>§</sup> T. C. Robbins is with the Department of Defense, Fort George G. Meade, MD 20755.

<sup>¶</sup> K. F. Galloway is with the Semiconductor Devices and Circuits Division, National Bureau of Standards, Washington, DC 20234, and the Electrical Engineering Department, University of Maryland, College Park, MD 20742.

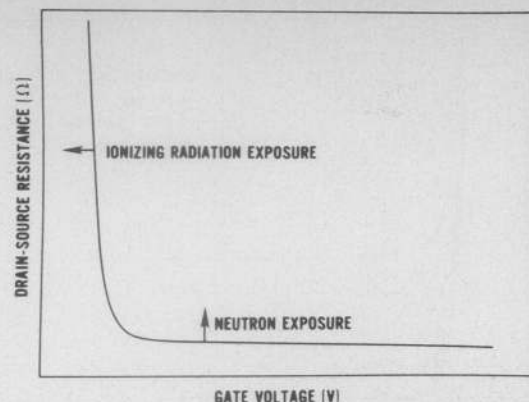


Figure 2. Plot of  $R_{DS}$  versus  $V_G$  as predicted by equation 1. The effects of ionizing and neutron irradiation on the relationship are indicated.

The principal effect of neutrons is on  $\rho_D$ , the drain region material resistivity. The resistivity increases due to the introduction of damage by the neutrons in the drain region. An empirical expression has been developed by Buehler relating the increase in resistivity to the neutron fluence.<sup>6</sup> For n-type silicon:

$$\rho_n = \rho_o \exp \frac{\phi}{444 \cdot n_o^{0.77}} \quad (2)$$

where  $\rho_n$  is the resistivity after exposure,  $\rho_o$  is the starting resistivity,  $\phi$  is the neutron fluence, and  $n_o$  is the starting dopant density.

Equation 2 predicts that the second term in equation 1 should increase exponentially with neutron fluence and that the magnitude of the increase should be greater the higher the starting resistivity (the smaller  $n_o$ ). Thus, the  $R_{DS}$  versus  $V_G$  relationship shifts vertically as a result of neutron irradiation (see figure 2).

#### Experimental Procedure

In order to illustrate the influence of radiation exposure (particularly neutrons) on the value of  $R_{DS}$  for VDMOS transistors, n-channel enhancement-mode devices with three different values of drain region material resistivity were used in this study. Approximately eight devices of each type were used in the study. The drain-source breakdown voltages of the devices which approximately reflect the value of  $\rho_D$  were used as a selection criteria for these devices. Table I lists the manufacturer's specified drain-source breakdown voltage and approximate dopant density ( $n_o$ ) and

Table I

Device Type	$BV_{DS}(V)^*$	$\rho_D(\Omega \cdot cm)^{**}$	$n_o(cm^{-3})^{**}$
A	450	~21	$\sim 2 \times 10^{14}$
B	350	~11 - 21	$\sim 2 - 4 \times 10^{14}$
C	150	~1.6	$\sim 3 \times 10^{15}$

\* Manufacturer's specified drain-source breakdown voltage.

\*\* Estimated from spreading resistance measurements.

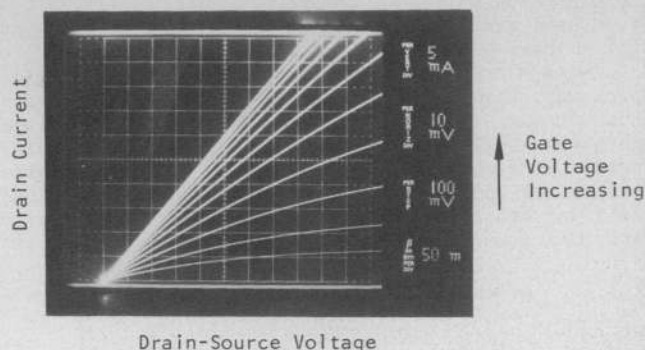


Figure 3. Curve tracer display of  $I_D$  versus  $V_{DS}$  as a function of  $V_G$ .  $V_G$  is offset by  $-3.6 V$ .

$\rho_D$  as estimated from spreading resistance measurements for each type.

The White Sands Missile Range Fast Burst Reactor was used for neutron irradiation tests. Devices were exposed to nominal neutron fluences of  $5 \times 10^{12}$ ,  $1 \times 10^{13}$ ,  $5 \times 10^{13}$ , and  $1 \times 10^{14}$  neutrons/cm<sup>2</sup> ( $E_n > 10$  keV). The neutron fluence was determined from measurements of sulfur pellets and a plutonium-sulphur ratio supplied by the facility. Calcium fluoride thermoluminescent dosimeters were utilized for dosimetry measurements of the ionizing radiation exposure accompanying the neutron fluence. For each neutron fluence level, the associated gamma irradiation was nominally  $1 \times 10^3$ ,  $2.4 \times 10^3$ ,  $1 \times 10^4$ , and  $2.2 \times 10^4$  rad(Si), respectively. In order to isolate the influence of gamma irradiation on the  $R_{DS}$  versus  $V_G$  relationship, the NBS Gamma Facility Co<sup>60</sup> Source<sup>7</sup> was used for supplementary ionizing radiation tests.

All of the neutron irradiations were done with the gate, drain, and source leads shorted to one another (i.e., the device was not under bias). Some gamma irradiation data were taken with a bias of  $+10 V$  between the gate and shorted source and drain leads.

Determinations of  $R_{DS}$  versus  $V_G$  were made using a curve tracer by measuring the drain current,  $I_D$ , versus  $V_G$  for a drain-source voltage of  $50 mV$ . The value of  $R_{DS}$  for each  $V_G$  was thus,  $R_{DS}(V_G) = 50 mV/I_D(V_G)$ . A photograph of a typical curve tracer CRT display is shown in figure 3. The value of  $V_{th}$  was estimated from plots of  $I_D$  versus  $V_G$  by extrapolating the most nearly linear region on the  $I_D$  versus  $V_G$  relationship to the  $I_D = 0$  intercept.<sup>8</sup> An example of this is shown in figure 4. One obtains only an estimate of  $V_{th}$  because of the existence of subthreshold current (current for  $V_G < V_{th}$ ) and because of the influence of the drain region resistance ( $F \cdot \rho_D$ ) on the  $I_D$  versus  $V_G$  relationship. The value of the estimated  $V_{th}$  is less than the true threshold voltage by about  $0.05$  to  $0.10 V$  for the unirradiated devices, but is estimated to be as much as  $0.3 V$  less after the devices experienced the highest neutron fluence.

#### Experimental Results and Discussion

Plots of  $R_{DS}$  versus  $V_G$  after successive levels of ionizing radiation exposure for a single device are shown in figure 5. The result is representative for all devices. As expected, for increasing levels of gamma irradiation, the  $R_{DS}$  versus  $V_G$  curves shift laterally to lower values of  $V_G$ . The shape of the relationship is essentially unchanged. Plots of the measured average change in  $V_{th}$  versus gamma irradi-

ation dose are shown in figure 6 for each device type with no bias applied and for type A with a bias of +10 V between their gate and shorted source-drain. For doses less than about  $10^4$  rad(Si), there is no difference between the shifts in  $V_{th}$  for the biased and unbiased devices. For larger doses a significantly greater shift occurs for the biased devices. These results are consistent with those presented by Bedingfield and Webster.<sup>9</sup> Because the gamma dose associated with the neutron fluence is usually less than  $10^4$

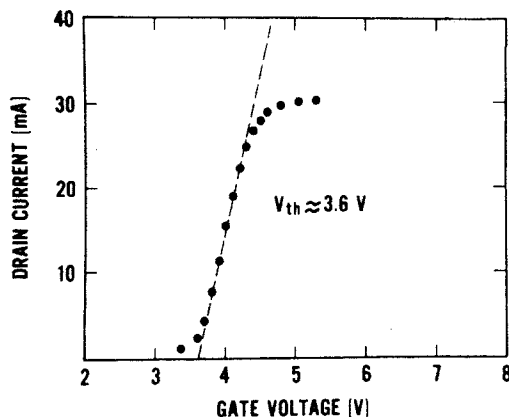


Figure 4. Plot of  $I_D$  versus  $V_G$  at  $V_{DS} = 50$  mV as determined from a display such as figure 3. The extrapolation of most nearly linear region to determine  $V_{th}$  is demonstrated.

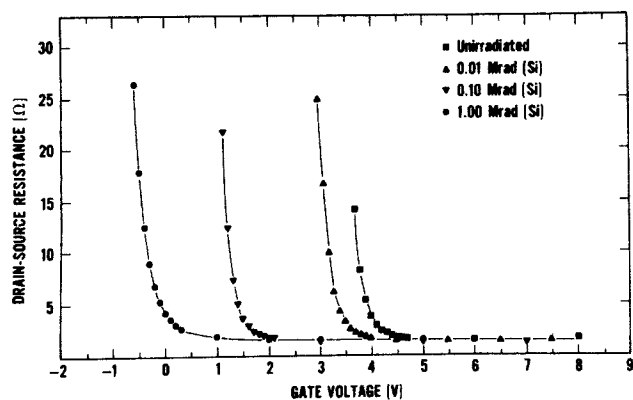


Figure 5. Example of effects of ionizing radiation on the  $R_{DS}$  versus  $V_G$  relationship.

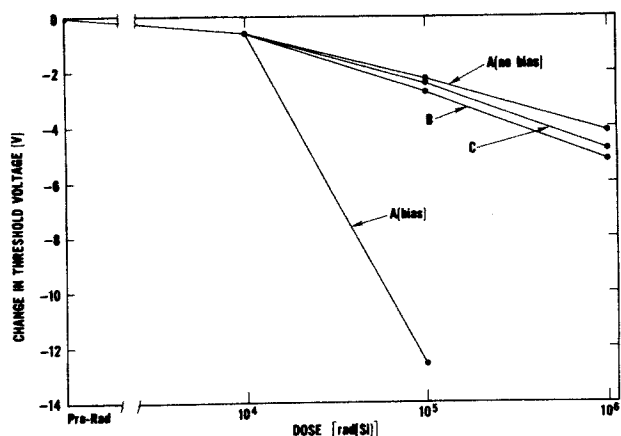


Figure 6. Measured average change in threshold voltage versus ionizing radiation dose.

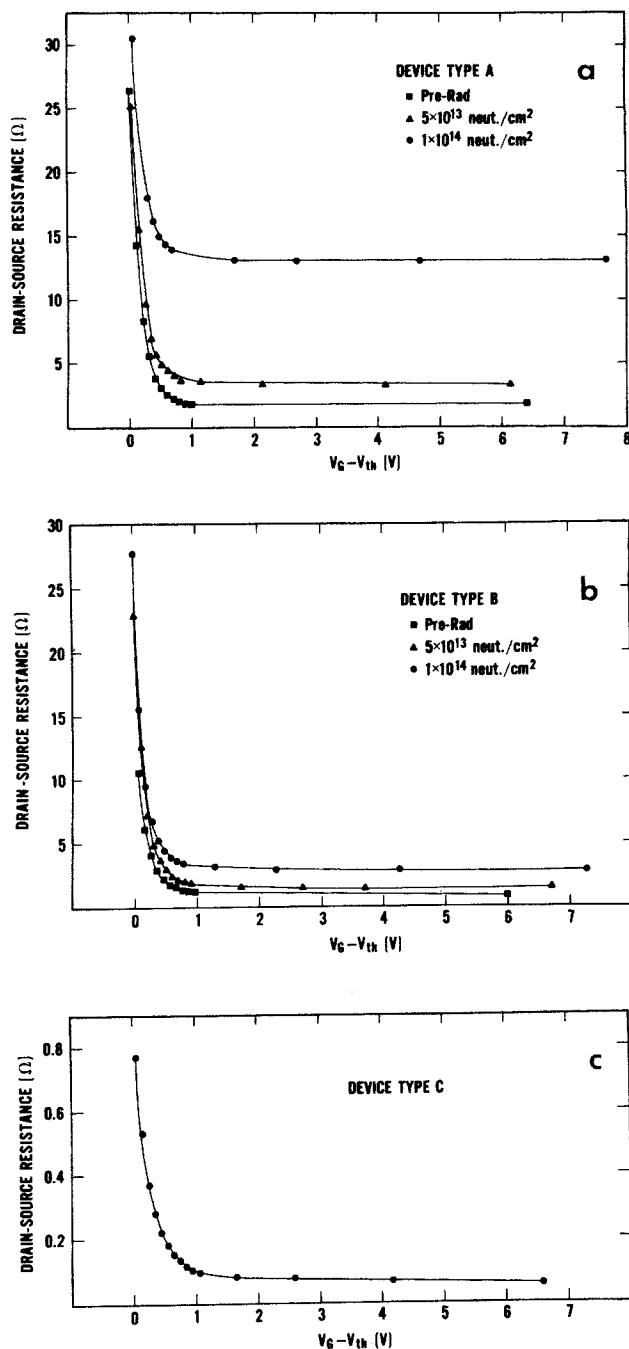


Figure 7. Example of effects of neutron irradiation on the  $R_{DS}$  versus  $V_G - V_{th}$  relationship. a), b), and c) are for a single device of types A, B, and C, respectively.

rad(Si), it is not expected that the presence of a gate bias would significantly affect the measured threshold shift after the neutron irradiation.

Plots of  $R_{DS}$  versus  $V_G - V_{th}$  after each level of neutron irradiation for a single device of each type studied are shown in figure 7. As expected, for increasing neutron dose, the curves shift vertically upward to larger values of  $R_{DS}$ . The shift is only vertical because the effect of the associated gamma irradiation, a lowering of  $V_{th}$ , is subtracted from  $V_G$  on the horizontal axis. Also, the relative increase in  $R_{DS}$  with neutron dose is larger, for larger values of  $\rho_D$ . For device type C, with the lowest value of  $\rho_D$ , no change in  $R_{DS}$  with neutron

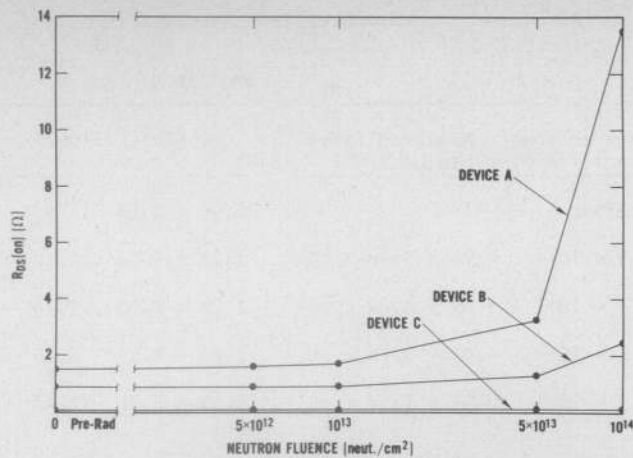


Figure 8. Plot of  $R_{DS(on)}$  versus neutron fluence level for each device type.

fluence level is observed. According to equation 2, no measurable change in  $R_{DS}$  should occur for device type C on exposure to the neutron levels used in this study.

A plot of the average  $R_{DS}$  values measured at  $V_G = 10$  V,  $R_{DS(on)}$ , for each device type for each level of neutron fluence is shown in figure 8.

Figures 5 to 8 indicate good qualitative agreement with the model previously discussed. There is, though, a large spread in measured  $R_{DS}$  values between devices of a given device type after the devices experienced the two highest neutron fluence levels. The data points in figure 9 represent the average value of  $R_{DS}$  and the error bars represent one standard deviation about the average for device types A and B. Data are shown for the two highest neutron fluence levels. Investigation of the quantitative agreement of the experimental results with the theoretical model is difficult because of the observed spread as well as a number of uncertainties. The major problems are:

1. The neutron fluence in the reactor is not spatially uniform. For each neutron dose level, each device does not experience the exact same level of irradiation. The sulfur pellets determine the irradiation level at the pellet location in the reactor and not at the location of each device. The neutron nonuniformity is greatest for the largest neutron dose.
2. For a given device type, the starting resistivity  $\rho_0$ , is not necessarily the same from device to device. The largest spread in  $\rho_0$  was found for device type B.
3. Spreading resistance measurements can be used only to estimate  $n_0(\rho_D)$ .
4. The theory relating  $\rho$  after neutron irradiation to  $\rho_0$  (equation 2) is empirical and is not expected to hold exactly for all values of  $\rho_D$  or all levels of neutron fluence.

There is evidence that the primary factor causing the large  $R_{DS}$  spread for device type A is the nonuniformity of neutron dose experienced by the devices and not variations in  $\rho_D$ . The value of  $R_{DS}$  measured at  $V_G = 10$  V ( $R_{DS(on)}$ ) is dominated by the second term in equation 1, so a measure of the variation in  $R_{DS(on)}$  should be an indicator of variations in

$\rho_D$ . The average value measured was  $1.47 \Omega$  with a standard deviation of  $\pm 0.04 \Omega$  (~3%). This suggests  $\rho_D$  was relatively constant from device to device. Also, spreading resistance measurements made on two devices indicated identical values of  $\rho_D$ . Variations of the neutron fluence should be reflected in the gamma irradiation levels; i.e., a high neutron fluence would be accompanied by a high gamma dose and conversely. Thus, the devices with the largest relative shifts in  $R_{DS}$  should also show the highest shifts in threshold voltage if variations in the neutron fluence caused the observed  $R_{DS}$  spread. A plot of the ratio of  $R_{DS(on)}$  after the highest neutron fluence level to the unirradiated  $R_{DS(on)}$  versus threshold voltage shift between the irradiated and unirradiated devices is shown in figure 10. There appears to be a correlation between the relative increase in  $R_{DS(on)}$  with the shift in threshold voltage for these devices. Thus the spread in  $R_{DS}$  for device type A at the highest neutron fluence can be attributed primarily to the variation in neutron fluence.

The results for device type B are complicated by an apparently large spread between devices in the unirradiated  $\rho_D$  values. The measured average  $R_{DS(on)}$  was  $0.99 \Omega$  with a standard deviation of  $\pm 0.16 \Omega$  (~16%) for

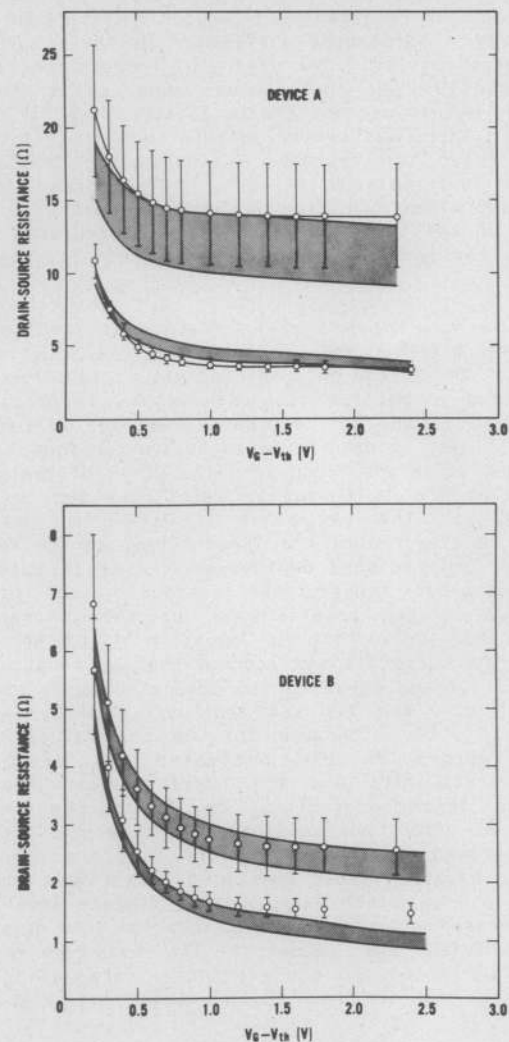


Figure 9. Experimental  $R_{DS}$  versus  $V_G - V_{th}$  results for two highest levels of neutron irradiation for device types A and B. The theoretical results are shown as a band superposed on the experimental results.

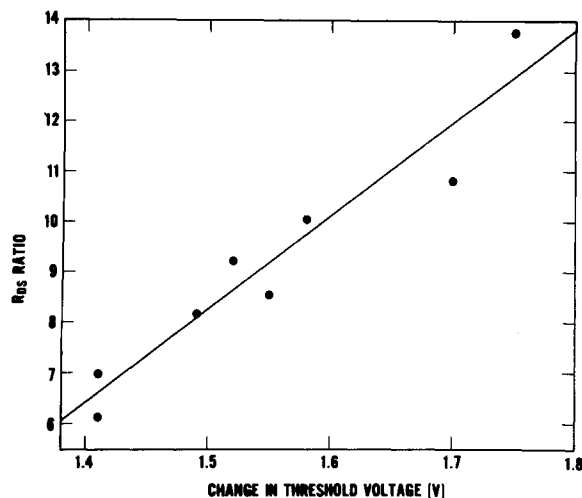


Figure 10. Plot of relative increase in  $R_{DS(on)}$  after highest neutron irradiation level versus change in threshold voltage for device type A.

the unirradiated devices. Two devices with a large difference in unirradiated  $R_{DS(on)}$  (1.10 and 0.81  $\Omega$ ) showed a 50-percent difference in their spreading resistance results. The degree of correlation between the relative  $R_{DS(on)}$  values and shift in  $V_{th}$  for this device was not nearly as strong as for device type A. There was better correlation for this device type between the relative  $R_{DS(on)}$  after irradiation and the unirradiated  $R_{DS(on)}$ . The spread in the  $R_{DS}$  results for the type B devices appears to be a result of the large spread in the unirradiated  $\rho_D$  as well as the nonuniformity of the neutron fluence levels.

In figure 9, a "band" of  $R_{DS}$  values as predicted by equations 1 and 2 are superposed on the experimental results. The spread in predicted values is a result of the spread in neutron fluence levels. To obtain the predicted curve, an estimated average value for  $\mu_e \cdot C_o \cdot W/L$  for these devices was determined. The estimated value was found from the slope of the linear portion of the  $I_D$  versus  $V_G$  relations used to estimate  $V_{th}$ . The value of  $\mu_e \cdot C_o \cdot W/L$  is assumed not to be affected by the irradiation, so the results from the unirradiated devices were used to determine this quantity. Next, the average values of  $R_{DS}$  versus  $V_G - V_{th}$  relationship for the unirradiated devices was curve fit to equation 1 to determine  $F \cdot \rho_D$ . The curve fit was accomplished by equating the measured average curve to the predicted curve at  $V_G - V_{th} = 1$  V. The fit was arbitrarily performed for  $V_G - V_{th} = 1$  V because for smaller values of  $V_G - V_{th}$  errors in the estimated  $V_{th}$  created a poor overall fit, and for larger values of  $V_G - V_{th}$  the dependence of  $\mu_e$  on  $V_G$  in the channel region, an effect not considered in this study, caused the experimental data to deviate from the predicted values. Equation 2 was then used to estimate the increase in  $F \cdot \rho_D$  after each neutron fluence level, and the increased value was used in equation 1 to determine the predicted  $R_{DS}$  values. The measured neutron fluence variation and the estimated average  $F \cdot \rho_D$  values after each neutron fluence level are listed in Table II.

To eliminate the effect of the spread in unirradiated  $\rho_D$  values for device type B, a group of four devices with nearly equal values of unirradiated  $R_{DS(on)}$  was chosen for the comparison. All of these devices had unirradiated  $R_{DS(on)}$  values in the range 0.81 to 0.84  $\Omega$ . A comparison of the measured average

Table II

TYPE A			
Neutron Dose (neut./cm <sup>2</sup> )	Measured Range (neut./cm <sup>2</sup> )	$F \cdot \rho_D (\Omega)$	$F \cdot \rho_D / F \cdot \rho_0$
Pre-Rad		$0.99 \pm 0.04$	1.00
$5 \times 10^{12}$	$4.99 - 5.46 \times 10^{12}$	$1.17 \pm 0.04$	1.18
$1 \times 10^{13}$	$1.19 - 1.22 \times 10^{13}$	$1.25 \pm 0.03$	1.26
$5 \times 10^{13}$	$4.63 - 5.79 \times 10^{13}$	$2.83 \pm 0.24$	2.86
$1 \times 10^{14}$	$0.98 - 1.17 \times 10^{14}$	$13.30 \pm 3.70$	13.43
$\mu_e \cdot C_o \cdot \frac{W}{L} = 0.744 \pm 0.025$			

TYPE B			
Pre-Rad		$0.37 \pm 0.06$	1.00
$5 \times 10^{12}$	$4.99 - 5.46 \times 10^{12}$	$0.40 \pm 0.08$	1.08
$1 \times 10^{13}$	$1.19 - 1.22 \times 10^{13}$	$0.46 \pm 0.08$	1.24
$5 \times 10^{13}$	$4.63 - 5.79 \times 10^{13}$	$0.90 \pm 0.14$	2.43
$1 \times 10^{14}$	$0.98 - 1.17 \times 10^{14}$	$2.11 \pm 0.46$	5.70
$\mu_e \cdot C_o \cdot \frac{W}{L} = 1.186 \pm 0.180$			

$R_{DS}$  for these four devices and the predicted  $R_{DS}$  spread is shown for the two highest levels of neutron fluence in figure 9b.

Considering the experimental uncertainties, the agreement of the experimental results and theoretical model is good. The experimental results indicate that  $R_{DS}$  saturates to a constant value for  $V_G - V_{th} > 1$  V, whereas the model predicts that  $R_{DS}$  should continue to decrease. The saturation of  $R_{DS}$  is probably because of the reduction of  $\mu_e$  in the inverted channel region at large values of  $V_G$ .

#### Summary and Systems Implications

The experimental data presented here on the drain-source resistance characteristics of power VDMOS transistors demonstrate that the change in  $R_{DS}$  with neutron exposure is related to the resistivity of the drain material, which in turn is related to the drain-source breakdown voltage.  $R_{DS(on)}$  increased by a factor of 13 for a 450-V device exposed to a neutron fluence of  $10^{14}/\text{cm}^2$ , while  $R_{DS(on)}$  for a 150-V device did not change at the same fluence. Ionizing radiation exposure resulted in threshold voltage shifts of about 2 V at  $10^5$  rad(Si) for the device types examined without bias, while positive bias during exposure accelerated the shift. The simple model for the dependence of drain-source resistance on gate voltage which can explicitly incorporate the effects of neutron exposure is in reasonable agreement with the experimental data.

The increase in  $R_{DS(on)}$  with exposure to high neutron fluence levels can have severe implications on the systems operation of VDMOS transistors. Because power dissipation increases in the on-state proportionally with  $R_{DS(on)}$ , the operating temperature of the

device will increase after neutron exposure. For a system which may experience a neutron environment, the heat-removal capabilities for the power MOSFET must be capable of handling the increased power dissipation. Also, the voltage and power capabilities of the drain power supply must be made large enough to properly bias the device with an increase in  $R_{DS(on)}$ .

The primary effect of the gamma irradiation is to shift  $V_{th}$  to lower values. In some instances, the  $V_{th}$  of these n-channel enhancement-mode devices can be shifted to negative values. In these instances, to turn the device off, a negative gate-source voltage must be applied to the device. The gate drive circuit must include the capability to supply a sufficient negative voltage to make sure the device can be turned off if the system is to be operated in an ionizing radiation environment.

The results of this study indicate that lot sampling would be appropriate for hardness assurance and survivability analysis if the lot has a tightly grouped  $R_{DS(on)}$  distribution. Otherwise, devices should be selected to yield such an  $R_{DS(on)}$  distribution. In addition one may conclude that the lower the unirradiated value of  $R_{DS(on)}$  for a device of a particular type, the harder that device is to neutron exposure.

#### Acknowledgments

The authors would like to acknowledge useful technical discussions with R. Bedingfield, T. Ellis, R. Pease, and C. Wilson, to thank W. Goodpaster and the WSMR FBR staff for assistance with the neutron irradiations, and to thank J. Ehrstein for performing the spreading resistance measurements. TCR would like to thank O. Van Gunten for making participation in this work possible. The authors would like to thank B. Yankey for her patience in the preparation of this manuscript.

#### References

1. R. Severns, "MOSFETs Rise to New Levels of Power," *Electronics* 53, No. 12, 143 (1980).
2. P. L. Hower, "A Comparison of Bipolar and Field-Effect Transistors as Power Switches," *Power Conversion International* 7, No. 1, 45 (1981).
3. W. E. Baker, Jr., "The Effects of Radiation on the Characteristics of Power MOSFETs," *Proc. POWERCON* 7, D3-1 (1980).
4. S. Rattner, "Additional Power VMOS Radiation Effects Studies," *IEEE Trans. Nucl. Sci.* NS-27, 1329 (1980).
5. S. C. Sun and J. D. Plummer, "Modeling of the On-Resistance of LDMOS, VDMOS, and VMOS Power Transistors," *IEEE Trans. Electron Devices* ED-27, 356 (1980).
6. M. G. Buehler, "Design Curves for Predicting Fast-Neutron-Induced Resistivity Changes in Silicon," *Proc. IEEE* 56, 1741 (1968).
7. J. C. Humphreys and W. L. McLaughlin, "Dye Film Dosimetry for Radiation Processing," *IEEE Trans. Nucl. Sci.* NS-28, 1797 (1981).
8. ASTM F 617 Standard Method for Measuring MOSFET Linear Threshold Voltage, *Annual Book of ASTM Standards*, Part 43, Philadelphia: American Society for Testing and Materials.
9. R. V. Bedingfield and W. E. Webster, Charles Stark Draper Laboratory Report C-5385 (1981).